Origin, formation and variability of the Subpolar Mode Water located over the Reykjanes Ridge

E. de Boisséson, V. Thierry, H. Mercier, G. Caniaux, D. Desbruyères

Origin, formation and variability of the Subpolar Mode Water located over the Reykjanes Ridge

E. de Boisséson,[1,2] V. Thierry,[1] H. Mercier,[3] G. Caniaux,[2] and D. Desbruyères[3]

Received 19 August 2011; revised 5 October 2012; accepted 16 October 2012; published 8 December 2012.

[1] The origin and formation of the Subpolar Mode Water (SPMW) located over the Reykjanes Ridge in the North-Atlantic Ocean and the variability of its properties over the period 1966–2004 are investigated through the use of a global eddy-permitting (1/4°) ocean/sea-ice model and a Lagrangian analysis tool. The SPMW is fed by subtropical and subpolar waters advected by the branches of the North-Atlantic Current. The SPMW acquires its properties when its source waters enter the winter mixed layer in the Iceland Basin. The SPMW temperature variability is mainly explained by variations of the relative contributions of the subtropical and subpolar water transports to the total transport. Compared to the 1966–2004 mean, lower (higher) subtropical water relative transport contribution leads to colder (warmer) SPMW in the early 1990s (in the late 1960s and late 1990s). The intensity of the winter convection in the Iceland basin also influences the SPMW temperature through the amount of relatively cold intermediate waters of subtropical origin integrated in the SPMW layer. Strong convection partly explains the cold SPMW of the early 1990s. The large increase in the SPMW temperature in the late 1990s is due to both a decrease in the winter convection and an increase in the relative transport of the subtropical waters.

Citation: de Boisséson, E., V. Thierry, H. Mercier, G. Caniaux, and D. Desbruyères (2012), Origin, formation and variability of the Subpolar Mode Water located over the Reykjanes Ridge, *J. Geophys. Res.*, *117*, C12005, doi:10.1029/2011JC007519.

1. Introduction

[2] The eastern subpolar gyre of the North Atlantic hosts waters from subpolar and subtropical origins that are advected by branches of the North Atlantic Current (NAC) (Figures 1 and 2). Among the upper waters of the eastern subpolar gyre, the Subpolar Mode Water (SPMW), formed in deep winter mixed layers, is identified by its nearly uniform thermohaline properties in the vertical direction near the top of the permanent pycnocline [*Hanawa and Talley*, 2001]. According to *Schmitz and McCartney* [1993] and *McCartney and Talley* [1982], the SPMW in the eastern subpolar gyre is expected to be advected toward the Labrador Sea and the Nordic Seas where it contributes to the formation of the deep waters of the overturning circulation. Various studies have shown that water masses of the eastern subpolar gyre in the depth range of the SPMW were subject to large interannual to decadal variability. The most recent prominent signal observed after the mid-1990s was a warming and a salinity increase that first occurred at the upper and intermediate levels [*Holliday et al.*, 2000; *Bersch*, 2002; *Holliday*, 2003; *Johnson and Gruber*, 2007; *Thierry et al.*, 2008; *Sarafanov et al.*, 2008; *Holliday et al.*, 2008]. This signal was then rapidly transferred to depths and might have influenced the intensity of the overturning circulation [*Sarafanov*, 2009; *Sarafanov et al.*, 2010].

[3] The origins of the upper ocean variability in the Northeast Atlantic have been the subject of numerous studies over the last 20 years. [*Reverdin et al.*, 1997] suggested that the decadal variability of the upper subpolar North Atlantic over the period 1948–1990 partly originated in the Labrador Sea from where temperature and salinity anomalies are advected to the eastern subpolar gyre by the NAC. By focusing on the Great Salinity Anomaly (GSA) events in the 1970s and 1980s, *Belkin et al.* [1998] also reported the propagation of temperature and salinity anomalies along the path of the NAC and secondary branches. *Holliday et al.* [2000] and *Holliday* [2003] invoked changes in the regional circulation as the main contribution to the warming and salinity increase of the upper waters of the Rockall Trough observed in the 1990s. Using an Ocean General Circulation Model (OGCM) based on the Miami Isopycnal Coordinate Ocean Model (MICOM), *Hátún et al.* [2005] found that changes in the local air-sea interactions and in the properties of the source waters were not responsible for the 1990s

[1]IFREMER, Laboratoire de Physique des Océans, UMR 6523, CNRS/IFREMER/IRD/UBO, Plouzané, France.
[2]Météo-France, CNRM-GAME, Météo-France/CNRS URA 1357, Toulouse, France.
[3]CNRS, Laboratoire de Physique des Océans, UMR 6523, CNRS/IFREMER/IRD/UBO, Plouzané, France.

Corresponding author: V. Thierry, Laboratoire de Physique des Océans, IFREMER/Centre de Brest, FR-29280 Plouzané, France. (virginie.thierry@ifremer.fr)

0148-0227/12/2011JC007519

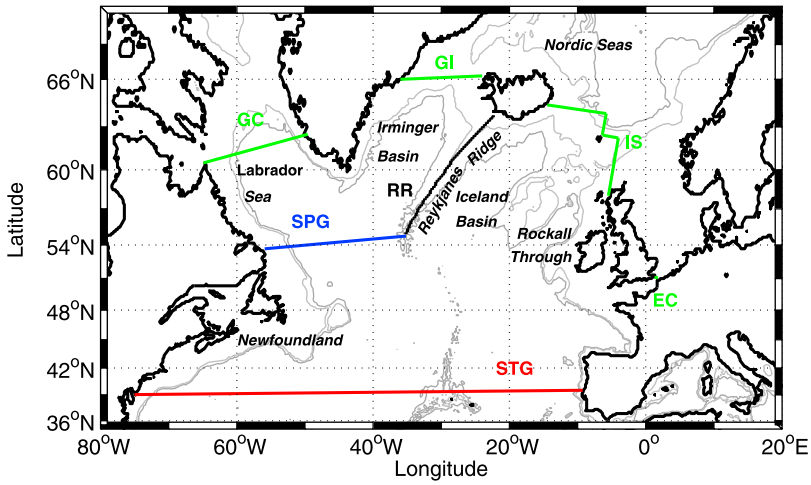

Figure 1. Map and bathymetry of the North-Atlantic Ocean. The gray lines are the 1000 and 2000 m isobaths. The black and colored thick lines are the initial and interception sections of the two Lagrangian experiments described in Section 4.1.

anomalously high salinities observed in the Rockall Trough, and in the Faroe and Irminger Currents. They showed that those salinity anomalies were mainly accounted for by the dynamics of the subpolar gyre circulation and its effects on the location, intensity, and composition of the NAC in the northeastern Atlantic. Focusing on the SPMW observed along 20°W [*Johnson and Gruber*, 2007] and over the eastern flank of the Reykjanes Ridge [*Thierry et al.*, 2008], *Johnson and Gruber* [2007] and *Thierry et al.* [2008] similarly suggested modifications in the relative contribution of subpolar (cold and fresh) and subtropical (warm and salty) water masses in the Iceland Basin as the most likely origin of the SPMW warming and salinity increase observed after the winter 1995/1996.According to *Johnson and Gruber* [2007] and *Sarafanov* [2009], this variability is related to the NAO (North-Atlantic Oscillation), the dominant mode of atmospheric variability in winter (December through March) in the North-Atlantic sector [*Hurrell*, 1995].

[4] Through the use of a global eddy-permitting ocean/sea-ice model at 1/4° resolution, the present study investigates the variability of the SPMW located over the Reykjanes Ridge, in a central position along the path of the subpolar gyre and where exchanges between the eastern and western parts of the gyre occur. This study complements *Thierry et al.*'s [2008] work that spanned the 1990s and early 2000s in providing a model description of the SPMW variability for the period 1966–2004. While the above-mentioned studies were conducted within an Eulerian framework, our investigation takes a Lagrangian point of view based on a backward tracking of SPMW particles advected by the model velocity field. The Lagrangian analysis [*Blanke and Raynaud*, 1997] is based on a numerical tool that was successfully used with different simulations by *Blanke et al.* [2002], *Lique et al.* [2010] and *Koch-Larrouy et al.* [2009] to quantify the water transports in various ocean basins. The Lagrangian analysis of SPMW particles in the model grid allows us to precisely determine their origins and their trajectories. By applying this method to the SPMW over the Reykjanes Ridge for the period 1966–2004, we expect to identify the mechanisms that play a key role in the variability of the SPMW properties.

[5] In the following, Section 2 describes the numerical simulation and the Lagrangian method. Section 3 evaluates the representation of the upper-ocean circulation and of the SPMW located over the Reykjanes Ridge in the model against observations. Section 4 describes the Lagrangian experiments performed for this study and investigates the origin and formation scheme of this SPMW. Section 5 depicts the SPMW variability and investigates the origin of this variability. Section 6 draws the conclusions of this study.

2. Numerical Simulation and Lagrangian Analysis Tool

2.1. The Numerical Experiment

[6] The numerical simulation used in this study is the ORCA025-G70 experiment performed in the framework of the Drakkar project [*Barnier et al.*, 2007]. The global ORCA025 model configuration at 1/4° resolution [*Barnier et al.*, 2006] is based on the NEMO (Nucleus for European Modeling of the Ocean) modeling framework [*Madec*, 2008]. The ORCA025-G70 experiment, fully described by *Treguier et al.* [2007] and *Molines et al.* [2006], was run from 1958 to 2004 with no prior spin up. The 5-day averaged model outputs provided a numerical ocean database. The initial condition was the Levitus 1998 climatology [*Levitus et al.*, 1998] for the low and mid latitude regions and the Polar Science Center Hydrographic Climatology (PHC) [*Steele et al.*, 2001] for the high latitude regions. The simulation used a global three-pole grid with 1442 × 1024 grid points and 46 vertical levels. The vertical grid spacing was finer near the surface (6 m) and increased with depth. The horizontal grid was isotropic and the resolution (1/4°) was 27.75 km at the Equator and 13.8 km at 60°N. Parameterizations included a Laplacian mixing of temperature and salinity along isopycnals, a horizontal biharmonic viscosity, and a turbulence closure scheme for vertical mixing

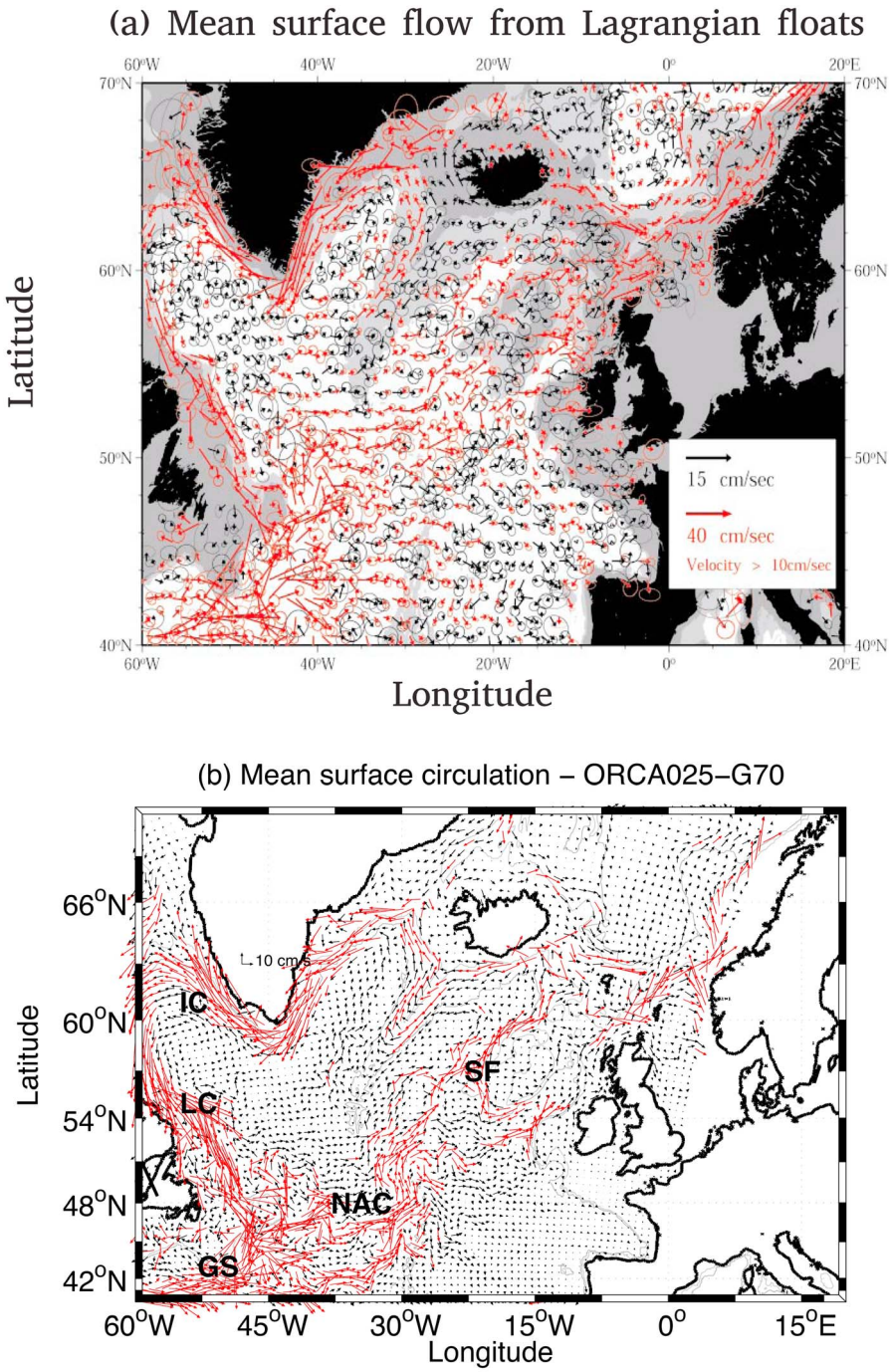

Figure 2. (a) The 1993–1998 mean circulation from Lagrangian floats (reprinted from *Flatau et al.* [2003]). (b) The 1993–1998 mean 16-m circulation in ORCA025-G70. GS, SF, LC, NAC and IC stand for Gulf Stream, Subarctic Front, Labrador Current, North Atlantic Current and Irminger Current, respectively. In the two panels, red arrows indicate velocities higher than 10 cm s^{-1}.

that is based on a prognostic equation for the turbulent kinetic energy and a closure assumption for the turbulent length scales [*Blanke and Delecluse*, 1993]. The surface forcing data set was a blend of data from various origins and at different time resolutions [*Brodeau*, 2007]. Precipitation and radiation were from the CORE (Common Ocean-ice Reference Experiments) data set [*Large and Yeager*, 2004] at monthly and daily frequency, respectively. Air temperature, humidity and wind speed were six-hour fields from the ECMWF (European Centre for Medium-Range Weather Forecasts) reanalysis ERA40 for the years 1958–2001 and from the ECMWF analysis for years 2002–2004. The turbulent fluxes (wind stress, latent and sensible heat fluxes) were estimated by application of the CORE bulk formulae

[*Large and Yeager*, 2004]. To prevent uncontrolled drift in salinity as a response to inaccurate precipitation [*Griffies et al.*, 2009], a relaxation to the Levitus/PHC climatology of sea surface salinity (SSS) was applied. The SSS restoring term is converted into an equivalent freshwater flux through a relaxation coefficient that was set to 0.17 meter per day. Considering the salinity evolution in the first vertical grid cell (6 m), the relaxation coefficient corresponded to a decay time of 36 days [*Molines et al.*, 2006] and led to a freshwater flux of similar amplitude as the one calculated from the forcing fields. There was also an extra restoring at the exit of the Red Sea and Mediterranean Sea to better represent their overflows.

2.2. The Lagrangian Analysis Tool ARIANE

[7] The Lagrangian analysis tool ARIANE (http://www.univbrest.fr/lpo/ariane/) is based on the algorithm developed by *Blanke and Raynaud* [1997]. Its initial purpose is to calculate trajectories of particles for a given three-dimensional (3D) stationary velocity field generated in averaging the time-varying velocity field of an ocean numerical model. The divergence is discretized on the model grid and allows the calculation of 3D streamlines within each box of the 3D mesh. For a stationary field, such streamlines are exact trajectories of particles in the model. This technique has been successfully extended to time-dependent velocity fields by assuming the velocity is stationary over successive periods equal to the available sampling [*Blanke and Raynaud*, 1997]. The present study uses 5-day averaged velocity field from the ORCA025-G70 simulation to advect particles over successive 5-day period.

[8] The resulting 3D trajectories represent the pathways followed by water parcels from an initial section of the ORCA025-G70 grid to several final interception sections. The small transport assigned to each particle at the initial section is conserved along the 3D trajectories. At each time step of their trajectories, the particles acquire the properties of the Eulerian ORCA025-G70 fields interpolated at the particle positions on the grid. Between two time steps, the particle properties are thus implicitly transformed through the influence of the atmospheric fluxes and the parameterized lateral and vertical mixing. Our experiments involved about 500000 particles seeded on one initial vertical section. The particle trajectories were then integrated backward in time to intersected sections to describe the upper subpolar North Atlantic circulation. The initial section was also an interception section. The particles were not uniformly distributed on the initial section. They are grouped in regions where the velocity is the highest ensuring that the particles carry the same transport. The methods for positioning the particles in the model grid and determining their transports are described in more details by *Blanke and Raynaud* [1997]. The maximum transport carried by a particle was set to 0.5 mSv, leading to a maximum error of 0.1 Sv on the transports computed at the intersected sections (1 Sv is defined as 1×10^6 m^3 s^{-1}). The vertical integration of the particle transports at each grid cell of the area enclosed by the sections provided a mean stream function describing the trajectory of the flow. Moreover, the vertical average of the particle properties at each grid cell provided an average view of the evolution of the particle properties along the mean trajectory of the flow (see Section 4).

3. SPMW in the Eastern Subpolar Gyre in ORCA025-G70

[9] This section describes the circulation in the model as well as the location and thermohaline properties of the SPMW in the eastern subpolar gyre as modeled by ORCA025-G70. The representation of the circulation and the SPMW in the model are evaluated against observations. This evaluation complements the one carried by *de Boisséson et al.* [2010] who used the ORCA025-G70 simulation to estimate a mixed layer heat budget in the Iceland Basin. They showed that despite an underestimated winter mixed layer depth, this simulation reproduced correctly the pattern and magnitude of the mean seasonal cycle of the heat content variation as estimated from Argo data.

3.1. Upper-Ocean Circulation

[10] The ORCA025-G70 circulation was averaged over the years 1993–1998 at 16 m depth (Figure 2) and over the years 1993–2001 on the 27.5 isopycnal (not shown) so as to be comparable with the 15-m circulation derived from drifter data [*Flatau et al.*, 2003] and with the circulation on the 27.5 isopycnal deduced from subsurface float data [*Bower et al.*, 2002]. The mean circulation highlights the flow of the NAC that is fed by the subpolar and subtropical gyres through the Labrador Current and the Gulf Stream, respectively. As in other realistic numerical models [*Smith et al.*, 2000; *Treguier et al.*, 2005], the NAC does not flow northward past Newfoundland before turning right and flowing eastward toward the Mid-Atlantic Ridge (MAR), along the Northwest Corner. Instead, it reaches the MAR and the Charlie Gibbs Fracture Zone through a more southerly path. The NAC then crosses the MAR and feeds the eastern subpolar gyre where it separates into three main branches (Figure 2) that flow through the Rockall Trough toward the Nordic Seas, along the western flank of the Rockall Plateau and through the central Iceland Basin, respectively. The last two branches partly feed the Nordic Seas and partly recirculate along the Reykjanes Ridge. A southwestward circulation along the eastern side of the Reykjanes Ridge is present in the model at 16-m depth and on the 27.5 isopycnal in agreement with floats-derived circulation at the same levels as reported by *Flatau et al.* [2003] (Figure 2) and *Bower et al.* [2002, Figure 3], and with ADCP measurements near 60°N [*Lherminier et al.*, 2007]. The southwestward flow recirculates around the Reykjanes Ridge and feeds the Irminger Current on the western side of the Reykjanes Ridge. In agreement with *Bower et al.* [2002], a small fraction of the NAC feeds the Irminger Current without flowing in the Iceland Basin.

[11] To evaluate the ability of ORCA025-G70 at simulating the amplitude and the timing of the variability of the North-Atlantic circulation, we calculated, following *Häkkinen and Rhines* [2004], the first empirical orthogonal function (EOF) of the sea surface height (Figure 3). The horizontal pattern and the principal component of this first EOF are in good agreement with those deduced from altimetry data over the satellite period [*Häkkinen and Rhines*,

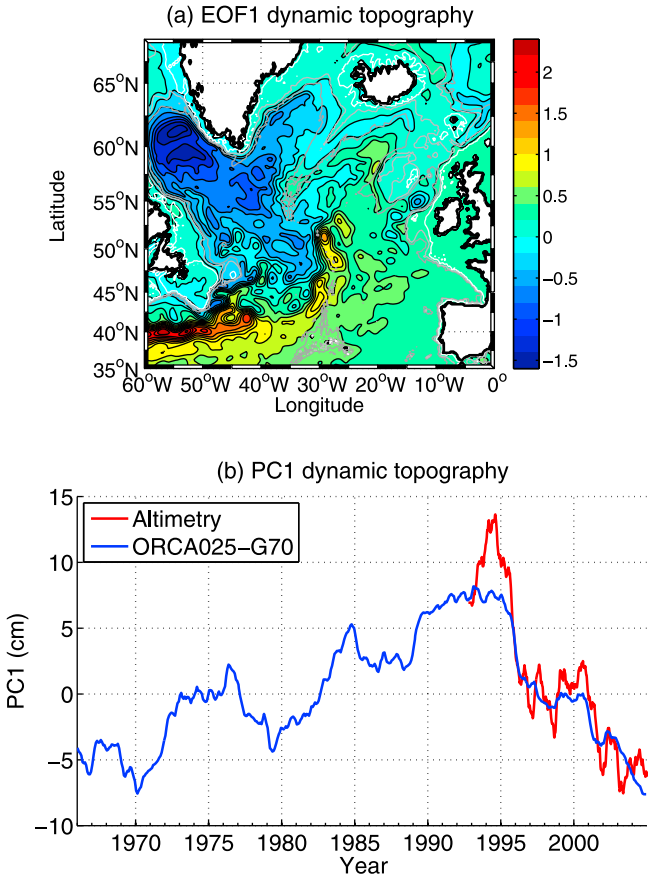

Figure 3. (a) First EOF of the sea surface height in ORCA025-G70 (24% of the variance). Contours of SSH anomalies have no units. The gray lines are the 1000 and 2000 m isobaths. (b) Temporal evolution of the corresponding principal component from ORCA025-G70 over 1966–2004 (blue curve) and from altimetry over 1993–2006 (red curve).

2004]. The correlation between the detrended time-series is 0.7 (significant at the 95% level) and the model is able to represent the high gyre index values observed in the early-1990s, the sharp decrease after the 1995–1996 winter and the continuous decreasing trend until the mid-2000s (Figure 3b). Moreover the long-term pattern of the gyre index estimated from ORCA025-G70 is comparable to that estimated by *Hátún et al.* [2005] from the MICOM simulation.

3.2. SPMW

3.2.1. Definition and Spatial Distribution

[12] In the following, the SPMW layer refers to the nearly-homogeneous water mass (excluding the Labrador Sea Water) bounded by the seasonal and the permanent thermocline. It is identified by a minimum of potential vorticity, ignoring relative vorticity [*Talley*, 1999; *Johnson and Gruber*, 2007; *Thierry et al.*, 2008; *Brambilla and Talley*, 2008]. As in *Johnson and Gruber* [2007] and in *Thierry et al.* [2008], the SPMW layer is defined by a potential vorticity lower than 6×10^{-11} m^{-1} s^{-1}, a salinity higher than 34.98 and a potential density lower than 27.7 kg m^{-3}. The core properties of the SPMW are the properties in the SPMW layer at the level where the potential vorticity is minimum. SPMW properties are estimated every year over the summer period (June to September) when mode waters are isolated from the atmosphere and their properties remain relatively stable. Each yearly estimate of the SPMW properties is referred to as a SPMW vintage in the following.

[13] The spatial distribution of the modeled SPMW and its density for June 1990 and June 2004 are shown on Figure 4. As in the observations [*Thierry et al.*, 2008; *Brambilla and Talley*, 2008], the SPMW in ORCA025-G70 are mainly found in the Rockall Trough, over the Rockall Plateau, in the East and the North of the Iceland Basin and over the Reykjanes Ridge. In the Iceland Basin, the main patches of SPMW are found on the warm sides of the three main branches of the NAC. Over the Reykjanes Ridge, the patch of SPMW is delimited by the southwestward and northeastward currents flowing along the eastern and western sides of the ridge (Figure 2). In 1990, the SPMW densities

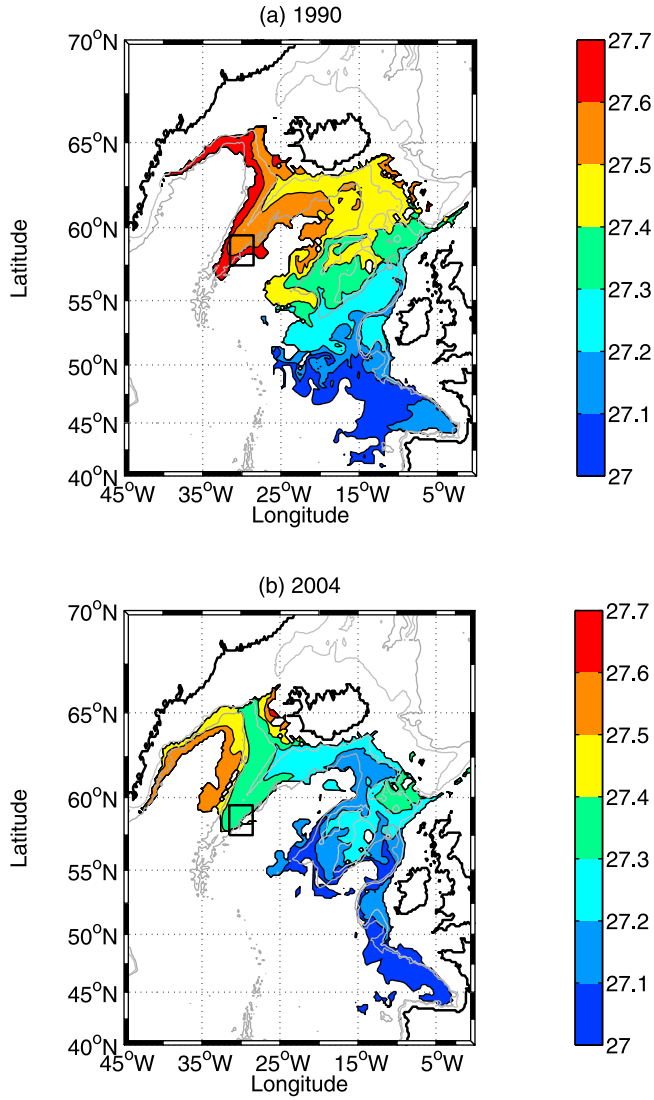

Figure 4. Potential density (in kg m^{-3}) in the core of the SPMW layer in (a) June 1990 and (b) June 2004 from the ORCA025-G70 outputs. The black box indicates the area where the average SPMW properties are plotted in Figure 5. The gray lines are the 1000 and 2000 m isobaths.

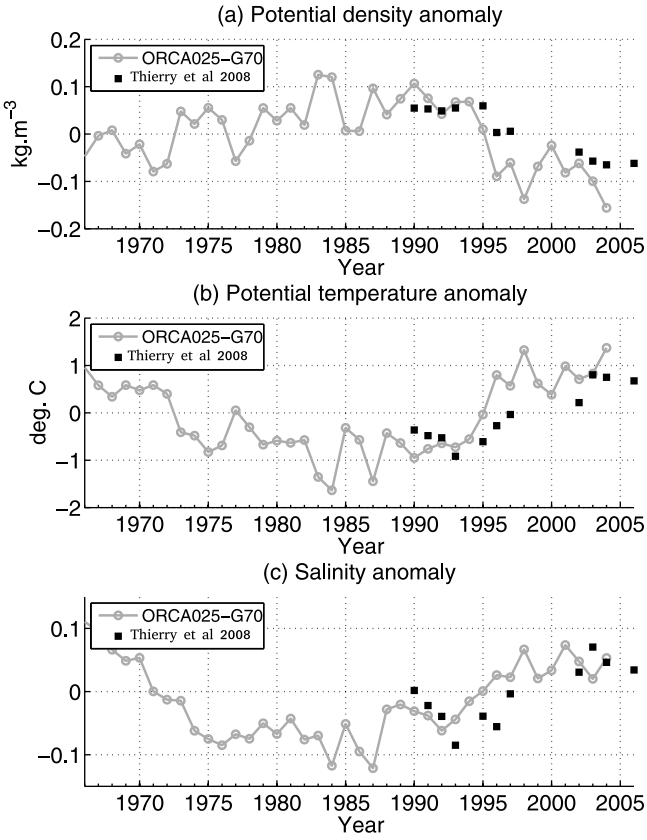

Figure 5. Anomalies of the core properties of the SPMW over the Reykjanes Ridge (located in the black box of Figure 4) in ORCA025-G70 for 1966–2004 period (gray line) and from observations for 1990–2006 (black squares) [*Thierry et al.*, 2008]. (a) Potential density, (b) potential temperature and (c) salinity. The mean properties calculated from the observations and ORCA025-G70 are 27.51 and 27.48 kg m^{-3} for density, 7.03 and 7.02°C for temperature, 35.12 and 35.09 for salinity, respectively.

increases northward from 27.0–27.1 to 27.4–27.5 kg m^{-3} in the Iceland Basin and the Rockall Through. Over the Reykjanes Ridge, the SPMW density is about 27.5 kg m^{-3}. Those values are in agreement with the 1900–2003 averaged values from *Brambilla and Talley* [2008]. In 2004, the SPMW densities are lower (by about 0.1 kg m^{-3}) and the spatial distribution of the SPMW is reduced compared to 1990, except in the Irminger Sea where the SPMW layer extends more to the west. A similar westward extension of the SPMW layer toward the eastern Irminger Basin was noticed by *Thierry et al.* [2008] when comparing 1992 and 2004 CTD data.

3.2.2. Variability

[14] Using in situ data, *Thierry et al.* [2008] described the variability over 1990–2006 of the SPMW properties in the 57.5–59.5°N/28.5–30.5°W box located on the eastern flank of the Reykjanes Ridge. The model-derived SPMW properties are averaged on a yearly basis over the same box for the period 1966–2004 (Figure 5). From the mid 1990s to the early 2000s, the temperature and the salinity of the SPMW in the model increased by about +1.5°C and +0.15 while the density decreased by 0.2 kg m^{-3}. This recent signal compares well with the warming of 1.4°C, the salinity increase of 0.11 and the decrease in density of 0.1 kg m^{-3} reported in *Thierry et al.* [2008]. From 1966 to 1975. the modeled SPMW cooled (−2°C) and freshened (−0.21). Then there was no clear trend until the early 1990s. Due to a lack of observations, it is not possible to directly evaluate the SPMW variability in the model over the 1966–1990 period. Instead, the ORCA025-G70 upper-layer (0–700 m) heat-content variability over 1966–2004 is compared to that from the World Ocean Database 2005 [*Boyer et al.*, 2006] in the Subpolar Gyre (51–66°N/65-5°W) (Figure 6). Despite the cold bias in the model at the beginning of the time-series, the model simulated the observed cooling of the upper-ocean from the mid-1960s to mid-1970s, the observed warming from the mid-1990s to the 2000s and the observed cold period in-between. The correlation between the two curves is 0.9. In this case and in the rest of the paper, detrended annual time series are considered and the correlation coefficients are only given when the correlation is significant at the 95% confidence level (p-value less than 0.05). The p-value is computed by transforming the correlation to create a t statistic following a t-Student distribution with N-2 degrees of freedom, where N is the number of points in the time series.

[15] The evaluation of the model against observations showed that the main characteristics of the SPMW (thermohaline properties, spatial distribution and variability) in the model are in reasonable agreement with the data. This suggests that the main mechanisms involved in the SPMW variability are represented in the model and justifies further investigation of the origin of the variability of the SPMW located over the Reykjanes Ridge. As the SPMW temperature variations are highly correlated with the SPMW salinity variations (correlation of 0.85) and anti-correlated with the SPMW potential density variations (correlation of −0.91)

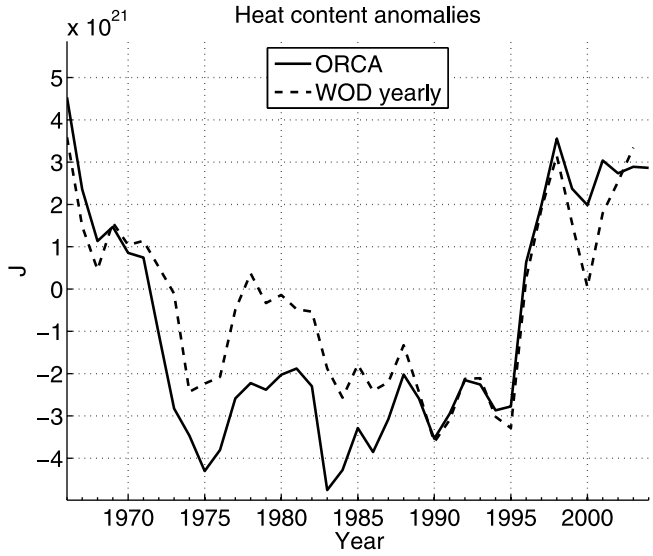

Figure 6. Yearly averaged upper ocean (0–700 m) heat content anomalies (in Joules) from ORCA025-G70 (plain line) over 1966–2004 and from the World Ocean Database 2005 over 1966–2003 (dashed line) in the Subpolar Gyre (51–66°N/65-5°W).

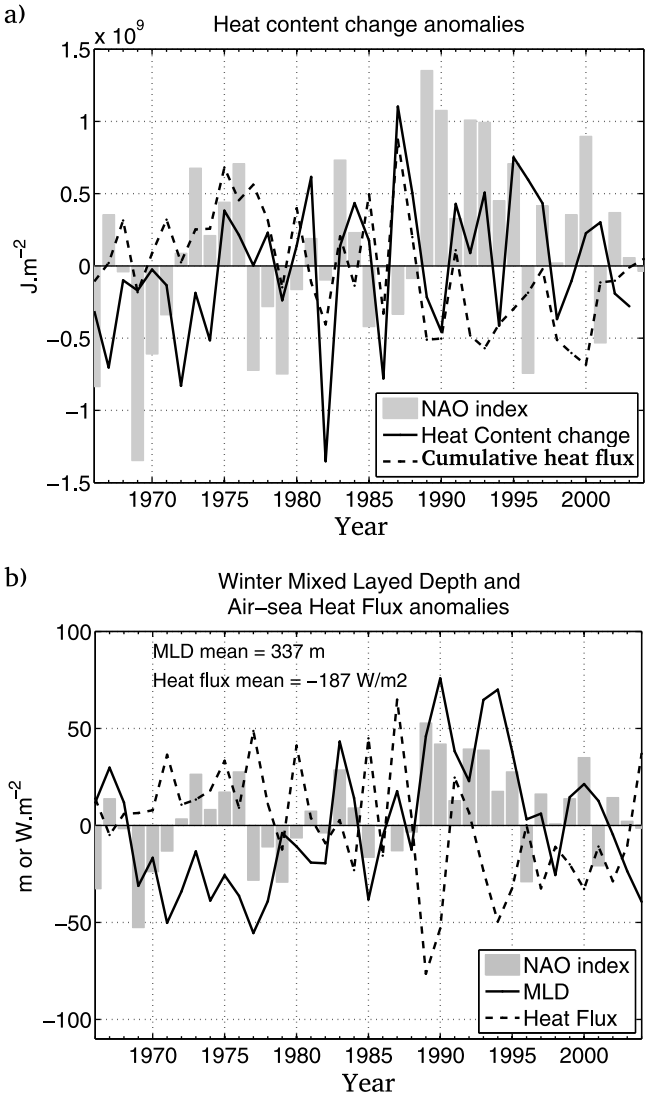

Figure 7. (a) Annual heat content anomalies in the 0–600 m layer in the Iceland Basin (between 54–63°N) (plain line) compared to changes in heat content due to air-sea fluxes (dashed line). (b) Winter mixed layer depth anomalies (in m, plain line) and winter heat flux anomalies (in W m^{-2}, dashed line) averaged in the Iceland Basin (between 54–63°N). The 1966–2004 mean was removed to the time-series and the winter NAO index is superimposed (gray bars) [*Hurrell*, 1995].

(Figure 5), we decided to focus the rest of the study on the SPMW temperature variability.

3.2.3. Role of the Surface Heat Fluxes

[16] Following *Holliday* [2003] and *Thierry et al.* [2008], local surface heat fluxes are compared to the heat content variations of the upper (0–600 m) south Iceland area in ORCA025-G70 (Figure 7). The correlation over the entire time-series between the heat content variations and the air-sea heat flux is not significant. While the annual regional air-sea heat flux contributed to the simulated changes of heat content in the 1980s, it cannot explain the variations that occurred before 1980 and after 1990 (Figure 7). Note that the freshwater flux cannot explain the variations of the freshwater content either (not shown). This suggests, as already hypothesized by other authors [e.g., *Hàtùn et al.*, 2005; *Johnson and Gruber*, 2007; *Thierry et al.*, 2008; *de Boisséson et al.*, 2010], that advection is a key mechanism to explain the variability of the water masses in the Iceland Basin. It justifies the use of a Lagrangian tool to investigate the variability of the SPMW over the Reykjanes Ridge, in particular through a better understanding of its origin and formation scheme.

4. Origin and Formation of the SPMW

4.1. Origin

[17] The Lagrangian experiments performed in this study were aimed to determine the origin of the SPMW located over the Reykjanes Ridge in summer (June to September). Two sets of experiments were performed in order to determine if the SPMW particles over the RR in the model originated in the Iceland Basin as suggested by the circulation scheme or if some contribution from west of the ridge exists. In both cases, the initial section, referred to as RR on Figure 1, was set along the top of the Reykjanes Ridge.

[18] The first experiment tracked SPMW particles flowing northwestward across the Reykjanes Ridge toward the Irminger Basin. Such particles were integrated backward in time until they reached one of the following sections: the RR section itself, the SPG section at the exit of the Labrador Sea, the STG section that crosses the Atlantic Ocean around 38°N, the EC section across the English Channel or the IS section along the Iceland-Scotland Ridge (Figure 1). The junction between the RR and SPG sections was chosen south of the region were the SPMW is found. In the following, the transports will be counted as positive towards the Irminger Basin across the RR section, northward across the STG section and southward across the SPG section. The integration was done over 8 years which ensured that at least 95% of the particles had reached one of the interception sections. This experiment was performed for SPMW vintages lying over the RR section every other summer from 1966 to 2004. The 8-year backward integration excluded the possibility of studying the SPMW vintages from the summer 1958 to 1965. Actually, 99% of the northwestward flowing SPMW particles had a subtropical or subpolar origin as they came either from the STG section or from the SPG section.

[19] The second experiment tracked SPMW particles flowing southeastward across the Reykjanes Ridge toward the Iceland Basin. The particles were integrated backward in time until they reached one of the following sections: the RR section itself, the SPG section, the GI section between Greenland and Iceland and the GC section across the Labrador Sea (Figure 1). The integration settings are the same as in the first experiment. The integration revealed that no particle originating from the SPG section, the Labrador Sea or the Nordic Seas feeds the SPMW layer on the Reykjanes Ridge. In fact, all the southeastward flowing particles originates from the southern part of the RR section and their transport is less than 0.1 Sv. Compared to the contribution of the northwestward flowing particles that varies between 2 and more than 6 Sv in the first experiment (Figure 8a), the southeastward flowing particles contribution to the SPMW layer is negligible and will not be taken into account in the rest of the study.

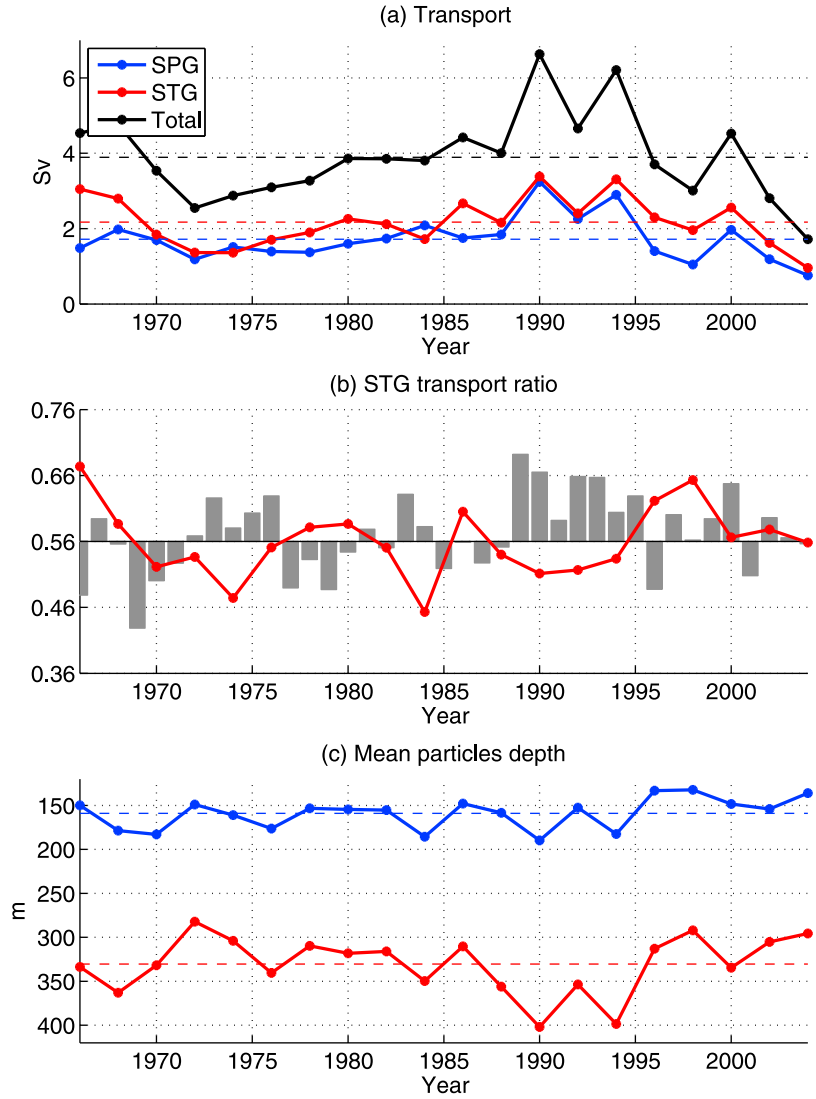

Figure 8. (a) Transport (in Sv) of SPMW particles across RR section during 1966–2004 (black curve). The transport of particles originating from the STG (Tr_{STG}) and SPG (Tr_{SPG}) sections are in red and blue, respectively. (b) Relative contribution (R_{STG}) of particles coming from the STG section to the total transport of SPMW particles across the RR section in 1966–2004 (red line) and winter NAO index (gray bars) [*Hurrell*, 1995]. (c) Averaged depth of the particles coming from the STG (in red) and SPG (in blue) sections. On Figures 8a and 8c, the dashed lines represent the mean values over 1966–2004 of each plotted variables.

[20] The Lagrangian experiments showed that, in ORCA025-G70, the SPMW over the Reykjanes Ridge was fed by the southwestward flow on the eastern flank of the ridge. Due to the relative coarse resolution of the model, the role of the Irminger Current through eddy mixing is not explicitly resolved and the influence of this term on the SPMW variability will not be assessed. However, we hypothesize that this mechanism is not of primary importance to explain the SPMW variability because of the good agreement between the observed and simulated SPMW variations. In addition, as the cyclonic subpolar gyre induces an overall westward circulation pattern in the Irminger Basin, the Irminger Current instabilities will preferentially influence, through eddy shedding, the Irminger Basin rather than the water masses on the Reykjanes Ridge [see *Bower et al.*, 2002, Figure 1].

[21] In the rest of the study, only particles crossing the Reykjanes Ridge toward the Irminger Basin and originating from either the STG or the SPG sections are considered. On average over 1966–2004, the mean northwestward transport of the SPMW particles across the RR section amounted to 3.9 Sv with 44.1% and 55.9% of the source particles coming from subpolar (section SPG) and subtropical (section STG) origins, respectively (Figures 8a and 8b). The SPMW transport decreased from the 1966 to the early 1970s and then increased to a maximum in 1990. It stayed high until the mid-1990s and then decreased, reaching its minimum in 2004.

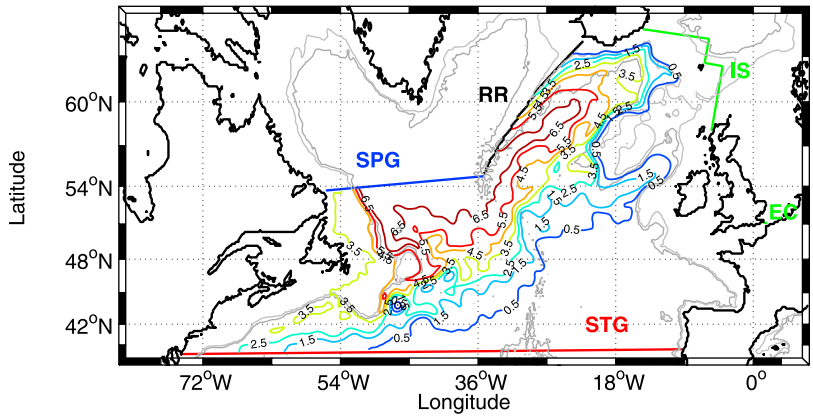

Figure 9. Mean stream function (in Sv) estimated by the Lagrangian tool ARIANE from the trajectories of particles that come from the STG and SPG sections and that feed the SPMW located over the Reykjanes Ridge during the summer 1990. The gray lines are the 1000 and 2000 m isobaths.

[22] Influenced by the air-sea fluxes and the lateral and vertical mixing along their trajectories, the subpolar particles generally gain heat from the SPG section to the RR section while the subtropical particles generally lose heat from the STG section to the RR section (not shown). The heat loss is larger than the heat gain and, on average over 1966–2004, the STG and SPG particles all considered are cooled by 0.8°C during their transit from the STG and SPG sections to the RR section. Indeed, the mean particle temperature, computed as indicated in Section 5.1, is 7.9 and 8.7°C at the RR and STG+SPG sections, respectively (not shown).

4.2. Formation

[23] The scheme of formation of SPMW located over the Reykjanes Ridge is now detailed. It is illustrated by the 1990 SPMW vintage because the mean stream functions followed by the source particles of the other SPMW vintages show very similar circulation patterns (not shown). According to the mean stream function provided by the Lagrangian experiment (Figure 9), two flows originating in the Labrador Current and the Gulf Stream merge off Newfoundland, cross the MAR between 48 and 52°N and enter the Iceland Basin where they feed the SPMW layer over the Reykjanes Ridge. The SPMW particles come from the STG and SPG sections on the west side of the MAR and follow a cyclonic pathway in the Iceland Basin (Figure 9). The travel time from the STG or SPG section to the RR section ranges from 2 to 4 years, the SPG-to-RR travel time being generally a few months shorter than the STG-to-RR travel time.

[24] In Figure 10, the 1990 mean stream function was superimposed on the mean potential vorticity of the particles after separating them in three temperature classes for a better visualization. This gives insight into position and time at which the particles enter the winter mixed layer before forming the SPMW layer at section RR. We consider that the particles are included either in the mixed layer or in the mode water layer when the mean potential vorticity is lower than the previously defined SPMW threshold 6×10^{-11} m^{-1} s^{-1}. Upstream of the Reykjanes Ridge, the particles reach this value in winter 1989/1990 while they are included in the deep mixed layers of the Iceland Basin (Figure 10). These weakly stratified waters are then advected toward the Reykjanes Ridge. It can be shown that the faster a particle flows, the further away from the Reykjanes Ridge it is included in the winter mixed layer. To conclude, the SPMW vintages are formed in the ocean mixed layer of the Iceland Basin from water parcels advected by the cyclonic circulation of the eastern subpolar gyre the winter before their summer transit above the Reykjanes Ridge.

[25] Despite the limitations of the model in representing some features of the regional horizontal circulation (see Section 3.1), the model-based scheme of origin and formation of the SPMW over the Reykjanes Ridge is consistent with the complementary observation-based studies of *Brambilla et al.* [2008] and *Thierry et al.* [2008]. *Brambilla et al.* [2008] showed that the source/product chain for SPMW formation in the eastern North-Atlantic is associated with the main branches of the NAC along which the SPMW is present and demonstrated that most of the diapycnal flux that creates the SPMW occurs in winter. *Thierry et al.* [2008] suggested a cyclonic circulation of the source waters in the Iceland Basin and a formation in the winter mixed layer close to the Reykjanes Ridge.

5. Variability of the SPMW

5.1. Variability at the RR and STG+SPG Sections

[26] Since the particle temperatures were known for a given Lagrangian experiment and because all particles had comparable transports (0.1 ± 0.04 mSv), we determined for each experiment, the mean temperature of the SPMW at the RR section (T_{RR}) as the arithmetic mean of the particle temperatures. We verified that T_{RR} is not different from the estimate using the weighted mean of the particle temperatures, the weights being the particle transports, which would be the exact formulation (Figure 11). Similarly, considering the STG and SPG sections together (referred to as the STG+SPG section in the following) and using the arithmetic mean temperatures of the particles in the STG (T_{STG}) and SPG (T_{SPG}) sections, the mean temperature of the STG+SPG section ($T_{STG+SPG}$, Figure 11) was computed as:

$$T_{STG+SPG} = T_{STG} \cdot \frac{Tr_{STG}}{Tr_{STG} + Tr_{SPG}} + T_{SPG} \cdot \frac{Tr_{SPG}}{Tr_{STG} + Tr_{SPG}} \quad (1)$$

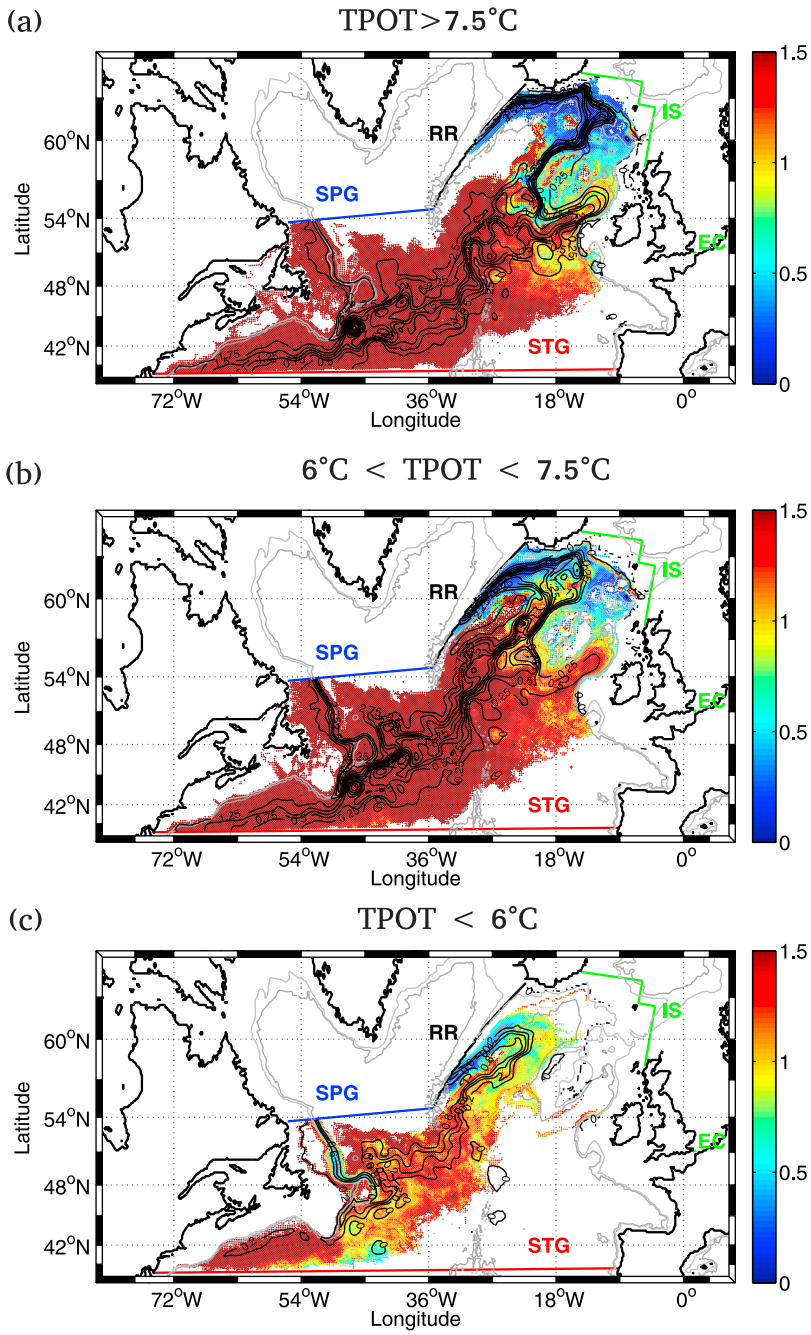

Figure 10. Mean potential vorticity along the trajectories of the particles that feed the SPMW located over the Reykjanes Ridge during the summer of 1990 for three temperature classes: (a) temperature greater than 7.5°C; (b) temperature comprised between 6 and 7.5°C; (c) temperature less than 6°C. The corresponding mean stream functions are superimposed. The gray lines are the 1000 and 2000 m isobaths.

Tr_{STG} and Tr_{SPG} are the transports of the particles originating from the STG and SPG sections, respectively (Figure 8a).

[27] Time series of the SPMW temperature averaged over the entire RR section showed a slow decrease of the SPMW temperature from the mid-1960s to the first half of the 1990s (−1.4°C) followed by a rapid increase (+1.7°C) until the mid-2000s (Figure 11). To help understand the origin of this variability, we compared the properties of the SPMW particles in the RR section with the properties of the same particles at their source in the STG+SPG section (Figure 11). In Figure 11, $T_{STG+SPG}$ was referenced to the year of particle seeding on the RR section and not to the year the particles were found on the STG or SPG sections because each individual particles had its own transit time between the two sections. Accordingly, despite the 2 to 4 years transit time between the STG or SPG sections and the RR section, there was no lag between T_{RR} and $T_{STG+SPG}$.

[28] Over 1966–2004, the averaged temperature in the STG+SPG section and in the RR section exhibited similar interannual to interdecadal variabilities. In particular, a

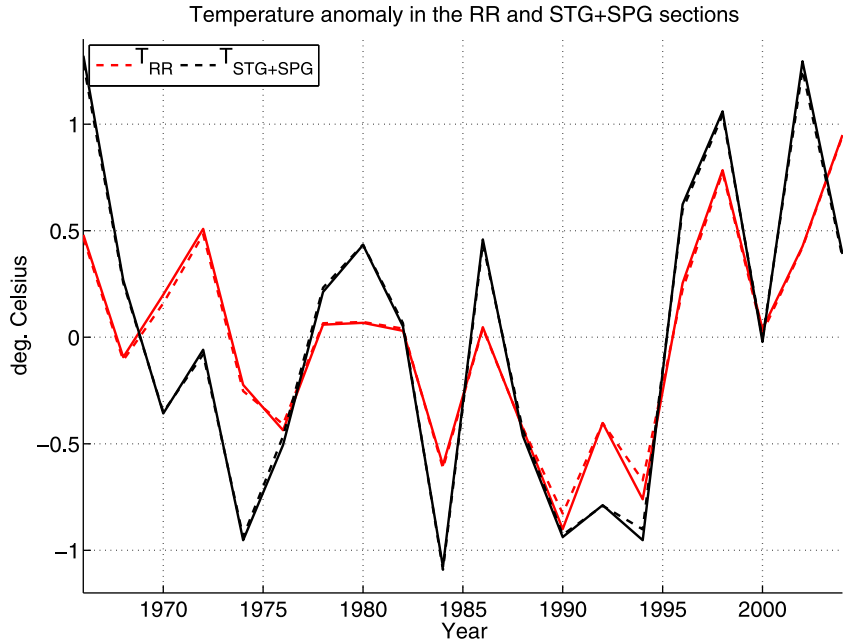

Figure 11. Anomalies of the mean particle temperature in the RR section (T_{RR}, black lines) and in the STG+SPG section ($T_{SPG+STG}$, red lines) over 1966–2004. The dashed lines represent the mean particle temperature computed in weighting the particle temperatures by the particle transports. The plain lines represent the approximate value of $T_{SPG+STG}$ and T_{RR} computed without taking into account the individual transport of each particles (see text for details).

similar abrupt increase of more than 1°C from the mid-1990s to the mid-2000s occurred at both sections. The correlation coefficients between the time-series of the particle temperature in the RR section and in the STG+SPG section was 0.80, which suggests that most of the signal in section RR was carried by the thermohaline properties of the particles originating from the STG and SPG sections. The amplitude of the variations was slightly smaller in the RR section compared to that in the STG+SPG section suggesting that the mixing and the air-sea fluxes tended to smooth the variability.

5.2. Terms Controlling the Variability

[29] Owing to equation (1), it was then possible to understand the variability carried by the STG and SPG particles. Each temperature term (T_{STG} and T_{SPG}) was decomposed as a mean value $\overline{T}$ over 1996–2004 and an anomaly T′. Similarly, the STG transport ratio $R_{STG} = Tr_{STG}/(Tr_{STG} + Tr_{SPG})$ was decomposed in a mean value $\overline{R_{STG}}$ over 1996–2004 and an anomaly R_{STG}. The SPG transport ratio $R_{SPG} = Tr_{SPG}/(Tr_{STG} + Tr_{SPG})$ equaled $R_{SPG} = 1 - R_{STG}$. Equation (1) then became after some algebra:

$$T_{STG+SPG} = T'_{STG}.\overline{R_{STG}} + T'_{SPG}.\overline{R_{SPG}} + \left(\overline{T_{STG}} - \overline{T_{SPG}}\right).R'_{STG} + \left(T'_{STG} - T'_{SPG}\right).R'_{STG} + constant \quad (2)$$

[30] The first two terms on the right hand side of equation (2) represent the influence of the varying temperature at the STG and SPG sections respectively in considering that the relative contributions of the STG and SPG transports to the total transport are constant and equal to 0.56 and 0.44 respectively (Figures 12a and 12b). The third term of equation (2) represents the influence of the varying contribution of the STG transport (and thus of the SPG transport) to the total transport (Figure 8b). The fourth term of equation (2) will not be considered in the rest of the study since it has negligible variations (*cross terms* curves on Figure 12c).

[31] The three main terms contributing to the temperature variations in the STG+SPG section varied on an interannual to interdecadal time scales. As seen on Figure 12c, the STG +SPG temperature variability was mainly controlled by the varying STG transport ratio with the noticeable exception of the early 1990s and early 2000s. In the early 1990s, the cold anomaly in $T_{STG+SPG}$ due to the reduced STG transport ratio was amplified by colder than usual STG particles (Figures 12a and 12c). At the beginning of the 2000s, the contribution of the STG transport ratio was not significant and the warm anomaly was explained by warmer than usual STG and SPG particles. $T_{STG+SPG}$ being strongly correlated with T_{RR} (0.80), those successive cold and warm anomalies led to the large SPMW temperature increase that occurred after 1994 (Figure 11).

5.3. Influence of the STG Particle Depth

[32] Over 1966–2004, the STG particle temperature variations around the temporal mean were less than 0.5°C except during 1990–1994 and in 2002, when a negative anomaly of about 0.5°C and a positive anomaly of about 1°C occurred, respectively (Figure 12). The STG temperature anomaly of the early 1990s is due to a larger contribution of deeper STG particles in 1990–1994 compared to the rest of the time series (Figure 8c). Indeed, these temperature anomalies disappeared when only particles at depths shallower than 350 m were considered in the STG section (T'_{STGup} curve on Figure 12). To illustrate this mechanism,

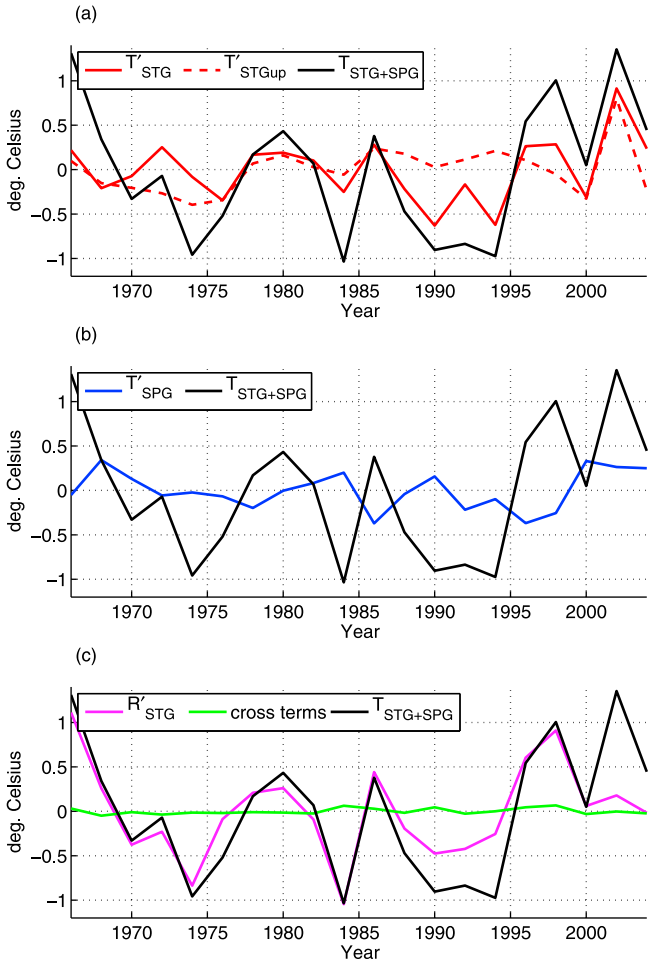

Figure 12. The anomaly of the averaged temperature of the future SPMW particles in the STG+SPG section (black plain line on all panels) is decomposed in four terms (see text for details) representing the contribution of (1) the varying properties of the STG particles (T_{STG}, red plain line on Figure 12a) or the varying properties of the STG particles when considering only particles shallower than 350 m in the STG section (T_{STGup}, red dashed lines on Figure 12a),

the 1970, 1990 and 1998 SPMW vintages were compared. The transport in depth bins of the particles in the STG section revealed that a larger number of particles from intermediate depths (350–800 m) contributed to the SPMW vintage in 1990 compared to 1970 and 1998 (Figure 13). Consequently, intermediate depth transport across the STG section of particles in the temperature range 5–10°C was higher in 1990 than in 1970 and 1998 (not shown) making the subtropical contribution to the SPMW cooler in 1990 than in 1970 and 1998 (Figure 12).

[33] To explain the changes in the averaged depth of the particles that fed the SPMW layer, we considered the time series of the winter mixed layer and winter heat flux averaged in the south Iceland area over 1966–2004 (Figure 7b). Over 1989–1995 (a prolonged positive NAO period), the winter heat loss was larger than its mean value and the winter mixed layer and the averaged particle depth in the STG section were deeper than their mean values (Figure 8c). The large heat loss of the early 1990s led to the intensification of the winter convection in the North-Iceland Basin and to the integration in the mixed layer - and thus in the future SPMW layer - of anomalously cold subtropical waters reflected by the extreme deep averaged particle depth in the STG section (Figure 8c). This also led to the formation of a larger volume of SPMW (not shown) and to an increase in STG particle transport (Figure 8a).

[34] Note that the mixed layer deepening in the Iceland Basin also influenced the SPG particles depth (Figure 8c) with however no significant signal in T'_{SPG} (Figure 12b) because of the relatively homogeneous vertical temperature profile at the SPG section.

6. Conclusion

[35] This study was aimed at investigating the origin and the formation of the SPMW lying over the Reykjanes Ridge and the mechanisms driving the variability of its properties in the ORCA025-G70 model. By tracking the SPMW particles back to their origin with the Lagrangian analysis tool ARIANE, we showed that the SPMW layer consisted of subpolar and subtropical water particles flowing with the NAC to the eastern subpolar gyre. On average, 44.1% and 55.9% of the particles originated from the Labrador Current (subpolar origin) and the Gulf Stream (subtropical origin), respectively (Figure 8). The SPMW located over the ridge acquired its properties a few months earlier in the Iceland Basin when its source waters entered the mixed layer during the winter convection (Figure 10). Those weakly stratified waters were then advected by the cyclonic circulation of the Iceland Basin toward the Reykjanes Ridge (Figure 9).

[36] In ORCA025-G70, the transport of SPMW particles across the Reykjanes Ridge increased from the early 1970s to the mid 1990s coinciding with a SPMW temperature decrease (Figures 8 and 11). The trends then reversed until the early 2000s. Most of the variability of the SPMW temperature over the Reykjanes Ridge was tracked back to the subtropical (STG) and subpolar (SPG) sections in terms of both particle temperature and transport variability. The variability of the SPMW temperature in the RR section was mainly due to the variations of the relative contribution of the STG and SPG particle transports to the total transport but occasionally variations of the particle temperature in the STG section (T_{STG}) also contribute to the total variability (early 1990s and 2000s) (Figure 12). The superimposition of both signals led to the variations of the SPMW temperature in the model. Particularly, the successive cold and warm anomalies of the SPMW temperature in the 1990s and 2000s induced an abrupt increase in the SPMW temperature of about 2.5°C that was also seen in the observations over 1990–2006 [*Thierry et al.*, 2008].

[37] Changes in the temperature of STG particles depended on the intensity of the winter convection in the Iceland Basin because it conditioned the respective volume of surface and intermediate waters that were integrated in the mixed layer and thus in the corresponding SPMW layer. In the early 1990s, when the mixed layer was deeper than during the early 1970s or the late 1990s, the strong winter convection integrated a larger amount of relatively cold intermediate waters in the SPMW layer and contributed to the cold STG particle anomaly occurring over that period (Figures 7, 8, and 13).

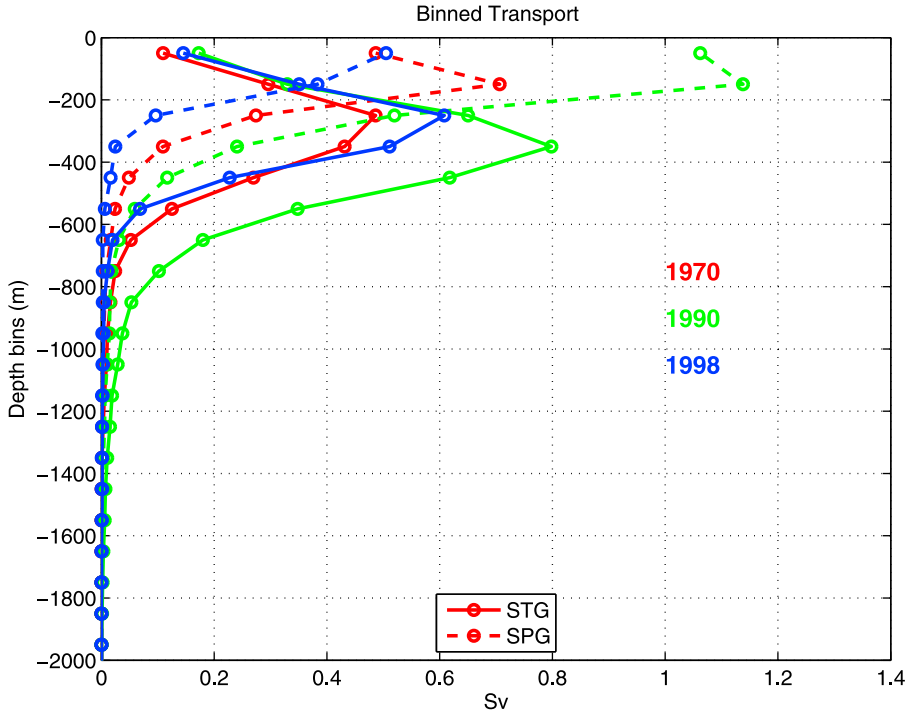

Figure 13. Binned transports (in Sv) according to the depth range of the future SPMW particles at their source on the SPG (dashed line) and STG (solid line) sections for the SPMW vintages of 1970 (red), 1990 (green) and 1998 (blue).

[38] The varying STG transport ratio R_{STG}, the main term controlling the SPMW variability, exhibited interannual to interdecadal variability (Figure 8b) that have some similarities with the interannual variations of the winter NAO index (the correlation coefficient is −0.52). For instance, R_{STG} was lower than its mean value during NAO-positive periods (1972–1976, 1982–1984 and 1988–1994). Although this is beyond the scope of this study, it is worth mentioning that understanding the relationship between R_{STG} and the NAO is challenging since the STG and SPG particle transports co-varied on the long term. Indeed, the STG and SPG particle transports are respectively influenced by the intensity of the co-varying subtropical and subpolar gyre transports [*Curry and McCartney*, 2001] and by the mixed layer deepening in the Iceland Basin.

[39] Results of the present study have potential implications for better understanding the causes of thermohaline changes at deeper levels in the subpolar gyre. First, the mode waters (and hence their properties) described in this paper are transported from the Northeast Atlantic to the Labrador Sea [*McCartney and Talley*, 1982], where wintertime convection overturns upper-ocean waters to depths down to ~2000 m [*Lazier et al.*, 2002]. Second, signals of temperature and variability in the northwestern Iceland Basin are directly transferred from the upper and intermediate levels to the deep ocean through entrainment of the Atlantic waters by the Iceland-Scotland Overflow Water [*Sarafanov*, 2009]. *Sarafanov et al.* [2010] found such transfer as the main cause of the rapid warming and salinity increase of the Iceland-Scotland Overflow Water since the mid-1990s. The question to what extent the mechanisms of the upper-ocean variability highlighted in the present study are involved in the deep-water thermohaline variability is thus a topic for future research.

[40] **Acknowledgments.** We sincerely thank three anonymous reviewers, Lynn Talley and the chief editor who contributed to improve the manuscript. The reading and comments of Artem Sarafanov were particularly appreciated. Eric de Boisséson is supported by IFREMER and Météo France, Virginie Thierry is supported by IFREMER, Herlé Mercier is supported by CNRS, Guy Caniaux is supported by Météo France and Damien Desbruyères is supported by CNRS and IFREMER. This is a contribution to the OVIDE project supported by IFREMER, CNRS, INSU and French national programs (GMMC and LEFE-IDAO).

References

Barnier, B., et al. (2006), Impact of partial steps and momentum advection schemes in a global ocean circulation model at eddy-permitting resolution, *Ocean Dyn.*, *56*, 543–567.

Barnier, B., et al. (2007), Eddy-permitting ocean circulation hindcasts of past decades, *Clim. Var. Predict. Exch. Rep. 42*, Int. CLIVAR Proj. Off., Southhampton, U. K.

Belkin, I. M., S. Levitus, J. Antonov, and S. A. Malmberg (1998), "Great Salinity Anomalies" in the North Atlantic, *Prog. Oceanogr.*, *41*, 1–68.

Bersch, M. (2002), North Atlantic Oscillation-induced changes of the upper layer circulation in the northern North Atlantic Ocean, *J. Geophys. Res.*, *107*(C10), 3156, doi:10.1029/2001JC000901.

Blanke, B., and P. Delecluse (1993), Low frequency variability of the tropical Atlantic Ocean simulated by a general circulation model with mixed layer physics, *J. Phys. Oceanogr.*, *23*, 1363–1388.

Blanke, B., and S. Raynaud (1997), Kinematics of the Pacific Equatorial Undercurrent: An Eulerian and Lagrangian approach from GCM results, *J. Phys. Oceanogr.*, *27*, 1038–1053.

Blanke, B., M. Arhan, A. Lazar, and G. Prévost (2002), A Lagrangian numerical investigation of the origins and fates of the salinity maximum water in the Atlantic, *J. Geophys. Res.*, *107*(C10), 3163, doi:10.1029/2002JC001318.

Bower, A. S., B. L. Cann, T. Rossby, W. Zenk, J. Gould, K. Speer, P. L. Richardson, M. D. Prater, and H.-M. Zhang (2002), Directly measured mid-depth circulation in the northeastern North Atlantic Ocean, *Nature*, *419*, 603–607.

Boyer, T. P., J. I. Antonov, H. E. Garcia, D. R. Johnson, R. A. Locarnini, A. V. Mishonov, M. T. Pitcher, O. K. Baranova and I. V. Smolyar (2006), *World Ocean Database 2005*, edited by S. Levitus, *NOAA Atlas NESDIS*, vol. 60, 190 pp., NOAA, Silver Spring, Md.

Brambilla, E., and L. D. Talley (2008), Subpolar Mode Water in the northeastern Atlantic: 1. Averaged properties and mean circulation, *J. Geophys. Res.*, *113*, C04025, doi:10.1029/2006JC004062.

Brambilla, E., L. D. Talley, and P. E. Robbins (2008), Subpolar Mode Water in the northeastern Atlantic: 2. Origin and transformation, *J. Geophys. Res.*, *113*, C04026, doi:10.1029/2006JC004063.

Brodeau, L. (2007), Contribution Ã l'Amélioration de la Fonction de Forçage des Modèles de Circulation Générale Océanique, PhD thesis, Univ. Joseph Fourier Grenoble 1, Grenoble, France.

Curry, R. G., and M. S. McCartney (2001), Ocean gyre circulation changes associated with the North Atlantic Oscillation, *J. Phys. Oceanogr.*, *31*, 3374–3400.

de Boisséson, E., V. Thierry, H. Mercier, and G. Caniaux (2010), Mixed layer heat budget in the Iceland Basin from Argo, *J. Geophys. Res.*, *115*, C10055, doi:10.1029/2010JC006283.

Flatau, M. K., L. D. Talley, and P. P. Niiler (2003), The North Atlantic Oscillation, surface current velocities and SST changes in the subpolar North Atlantic, *J. Clim.*, *16*, 2355–2369.

Griffies, S. M., et al. (2009), Coordinated Ocean-ice Reference Experiments (COREs), *Ocean Modell.*, *26*, 1–46, doi:10.1016/j;ocemod.2008.08.007.

Häkkinen, S., and P. B. Rhines (2004), Decline of subpolar North Atlantic circulation during the 1990s, *Science*, *304*, 555–559.

Hanawa, K., and L. D. Talley (2001), Mode waters, in *Ocean Circulation and Climate*, edited by G. Siedler, J. Church, and J. Gould, pp. 373–386, Academic, San Diego, Calif.

Hàtùn, H., A. B. Sando, H. Drange, B. Hansen, and H. Valdimarsson (2005), Influence of the Atlantic subpolar gyre on the thermohaline circulation, *Science*, *309*, 1841–1844, doi:10.1126/science.1114777.

Holliday, N. P. (2003), Air-sea interaction and circulation changes in the northeastern Atlantic, *J. Geophys. Res.*, *108*(C8), 3259, doi:10.1029/2002JC001344.

Holliday, N. P., R. T. Pollard, J. F. Read, and H. Leach (2000), Water mass properties and fluxes in the Rockall Trough, 1975–1998, *Deep Sea Res., Part I*, *47*, 1303–1332.

Holliday, N. P., et al. (2008), Reversal of the 1960s to 1990s freshening trend in the northeast North Atlantic and Nordic Seas, *Geophys. Res. Lett.*, *35*, L03614, doi:10.1029/2007GL032675.

Hurrell, J. W. (1995), Decadal trends in the North Atlantic Oscillation: Regional temperatures and precipitation, *Science*, *269*, 676–679.

Johnson, G. C., and N. Gruber (2007), Decadal water mass variations along 20°W in the northeastern Atlantic Ocean, *Prog. Oceanogr.*, *73*, 277–295, doi:10.1016/j.pocean.2006.03.022.

Koch-Larrouy, A., G. Madec, B. Blanke, and R. Molcard (2009), Water mass transformation along the Indonesian throughflow in an OGCM, *Ocean Dyn.*, *58*, 289–309, doi:10.1007/s10236-008-0155-4.

Large, W., and S. Yeager (2004), Diurnal to decadal global forcing for ocean and sea-ice models: The data sets and flux climatologies, *NCAR Tech. Note NCAR/TN460+STR*, Natl. Cent. for Atmos. Res., Boulder, Colo. [Available at http://nldr.library.ucar.edu/repository/collections/TECH-NOTE-000-000-000-601.]

Lazier, J., R. Hendry, A. Clarke, I. Yashayaev, and P. Rhines (2002), Convection and restratification in the Labrador Sea, 1990–2000, *Deep Sea Res., Part I*, *49*, 1819–1835.

Levitus, S., T. P. Boyer, M. E. Conkright, T. O'Brien, J. Antonov, C. Stephens, L. Stathoplos, D. Johnson, and R. Gelfeld (1998), *World Ocean Database 1998*, vol. 1, *Introduction*, *NOAA Atlas NESDIS*, vol. 18, 346 pp., NOAA, Silver Spring, Md.

Lherminier, P., H. Mercier, C. Gourcuff, M. Alvarez, S. Bacon, and C. Kermabon (2007), Transports across the 2002 Greenland-Portugal Ovide section and comparison with 1997, *J. Geophys. Res.*, *112*, C07003, doi:10.1029/2006JC003716.

Lique, C., A. M. Treguier, B. Blanke, and N. Grima (2010), On the origins of water masses exported along both sides of Greenland: A Lagrangian model analysis, *J. Geophys. Res.*, *115*, C05019, doi:10.1029/2009JC005316.

Madec, G. (2008), NEMO ocean engine, *Notes Pôle Model. Inst. Pierre-Simon Laplace 27*, 300 pp., IPSL, Paris, France.

McCartney, M. S., and L. D. Talley (1982), The Subpolar Mode Water of the North Atlantic Ocean, *J. Phys. Oceanogr.*, *12*, 1169–1188.

Molines, J. M., B. Barnier, T. Penduff, L. Brodeau, A. M. Treguier, S. Theetten, and G. Madec (2006), Definition of the interannual experiment ORCA025-G70, 1958–2004, *Rep. LEGI-DRA-2-11-2006i*, Lab. des Ecoulements Geophys. et Ind., Grenoble, France. [Available at http://www.drakkar-ocean.eu/publications/reports/orca025_G70.pdf/view.]

Reverdin, G., D. Cayan, and Y. Kushnir (1997), Decadal variability of hydrography in the upper northern North Atlantic in 1948–1990, *J. Geophys. Res.*, *102*(C4), 8505–8531.

Sarafanov, A. (2009), On the effect of the North Atlantic Oscillation on temperature and salinity of the subpolar North Atlantic intermediate and deep waters, *ICES J. Mar. Sci.*, *66*, 1448–1454, doi:10.1093/icesjms/fsp094.

Sarafanov, A., A. Falina, A. Sokov, and A. Demidov (2008), Intense warming and salinification of intermediate waters of southern origin in the eastern subpolar North Atlantic in the 1990s-mid-2000s, *J. Geophys. Res.*, *113*, C12022, doi:10.1029/2008JC004975.

Sarafanov, A., H. Mercier, A. Falina, A. Sokov, and P. Lherminier (2010), Cessation and partial reversal of deep water freshening in the northern North Atlantic: Observation-based estimates and attribution, *Tellus, Ser. A*, *62*, 80–90, doi:10.1111/j.1600-0870.2009.00418.x.

Schmitz, W. J., and M. S. McCartney (1993), On the North Atlantic circulation, *Rev. Geophys.*, *31*, 29–49.

Smith, R. D., M. E. Maltrud, F. O. Bryan, and M. W. Hecht (2000), Numerical simulation of the North Atlantic Ocean at 1/10°, *J. Phys. Oceanogr.*, *30*, 1532–1561.

Steele, M., R. Morley, and W. Ermold (2001), PHC: A global ocean hydrography with a high quality arctic ocean, *J. Clim.*, *14*, 2079–2087.

Talley, L. (1999), Antarctic Intermediate Water in the South Atlantic, in *The South Atlantic: Present and Past Circulation*, edited by G. Wefer et al., pp. 219–238, Springer, New York.

Thierry, V., E. de Boisséson, and H. Mercier (2008), Interannual variability of the Subpolar Mode Water properties over the Reykjanes Ridge during 1990–2006, *J. Geophys. Res.*, *113*, C04016, doi:10.1029/2007JC004443.

Treguier, A. M., S. Theetten, E. Chassignet, T. Penduff, R. Smith, L. Talley, J. O. Beismann, and C. Boening (2005), The North Atlantic subpolar gyre in four high-resolution models, *J. Phys. Oceanogr.*, *35*, 757–774.

Treguier, A. M., M. H. England, S. R. Rintoul, G. Madec, J. L. Sommer, and J. M. Molines (2007), Southern Ocean overturning across streamlines in an eddying simulation of the Antarctic Circumpolar Current, *Ocean Sci.*, *3*, 491–507.